AD-760 019

SEGMENTED HIGH AVERAGE POWER Ho(3+):YLF LASER

William C. Fricke

Sanders Associates, Incorporated

Prepared for:

Office of Naval Research
Advanced Research Projects Agency

10 May 1973

FINAL TECHNICAL REPORT (YPS)
For
SEGMENTED HIGH AVERAGE POWER
Ho^{3+}:YLF LASER
10 MAY 1973

Period Covered: 8 November 1971 - 31 December 1972

Contract No.: N00014-72-c-0137
Expiration Date: 31 December 1972
Amount of Contract: $82,353

Sponsored by
Advanced Research Projects Agency
ARPA Order No. 1806

Monitored by
Office of Naval Research - Department of the Navy
Program Code No. 421

Scientific Officer
Director, Physics Programs
Physical Sciences Division
Office of Naval Research, Department of the Navy
800 North Quincy Street
Arlington, Virginia 22217

This research was supported by the Advanced Research Projects Agency of the Department of Defense and was monitored by ONR under Contract No. N00014-72-c-0137.

SANDERS ASSOCIATES, INC.*
95 CANAL STREET NASHUA, NEW HAMPSHIRE

Principal Investigator: William C. Fricke
Phone No. (603) 885-3980

*T.M. Sanders Associates, Inc.

TABLE OF CONTENTS

TABLE OF CONTENTS (Cont.)

LIST OF ILLUSTRATIONS

LIST OF ILLUSTRATIONS (CONT)

ABSTRACT

The objective of this program was to prove the feasibility of using FEP Teflon(R) as a transparent solder in high average power disk lasers. This technique is aimed at reducing or eliminating the two major residual sources of beam distortion in such "sliced" laser configurations:

(a) Stresses in the disk, resulting from imperfect contact with the disk holder; and

(b) Radial Heat Flow by thermally insulating the edge of the disk.

By developing a method for cladding the laser disks with FEP Teflon(R) we have successfully shown that:

(a) Stresses in the disk can be completely eliminated; and,

(b) Radial Heat Flow and the resulting distortions can be reduced by approximately a factor of five over typical disk laser configurations.

To evaluate the effectiveness of this holding technique using FEP Teflon(R), a Nd:Glass disk array, incorporating many of the good features of current disk lasers has been built. Thermal, optical and mechanical measurements have been performed on the individual disks and on the array.

We have also determined that a CW Ho:YLF[1] disk laser similar to the Nd:Glass device built on this program would have a threshold of 22W/cm^3 and would produce 6W/cm^3 of output power. Repetitively Q switching at 50Hz would yield peak powers of 300MW/cm^3 (10 Joules in a 30ns wide pulse).

FORWARD

This program was carried out to determine the feasibility of a new concept for holding laser disks. This concept, whereby the disks are bonded into a disk holder with FEP Teflon$^{(R)}$, is based on an original idea of Dr. V. O. Nicolai. The technique for actually bonding the disk into the holder was developed at Sanders under this contract.

The author wishes to acknowledge the efforts of Dr. A. Linz of the MIT Center for Materials Science and Engineering and Department of Electrical Engineering to supply the Ho^{3+}:YLF crystals. The assistance and encouragement from both Dr. C. Naiman and D. S. Young has been greatly appreciated.

Section 1

INTRODUCTION

Disk lasers have greatly improved the average output power and beam quality of glass and other low conductivity laser hosts. Existing devices can generate beams with two orders of magnitude improvement in beam quality over their solid rod counterparts. Distortion, thermal lens effect and stress birefringence are still present and can be attributed to two sources - nonuniform pumping and nonuniform cooling. The result of both of these nonuniformities is heat flow in the radial direction. This, in turn, establishes radial variations in the index of refraction producing thermal lensing and stress inside the disk.

Nonuniform pumping can be easily corrected by well known procedures[2,3] which will not be discussed further here. Nonuniform cooling and its reduction or elimination, however, is one of the objectives of this program. Nonuniform cooling can produce beam walkoff, non-spherical thermal lens effects[4,5] and the associated stresses in the disks[6]. Beam walkoff occurs when the flow direction is the same across all the disks. The temperature at the inlet side of the disk is lower than at the outlet side of the disk and a temperature gradient and an optical wedge are established along the flow direction. This optical wedge is easily prevented[4] by alternating the flow direction from disk to disk (see Figure 1). Normally, a series/parallel flow path is employed to reduce the pressures necessary to produce the required flow rate.

Another form of nonuniform cooling occurs near the edge of the disk. If the coolant comes in contact with the edge of the disk, heat will flow radially outward. Such radial heat flow will produce edge effects similar to those produced throughout a solid rod. In

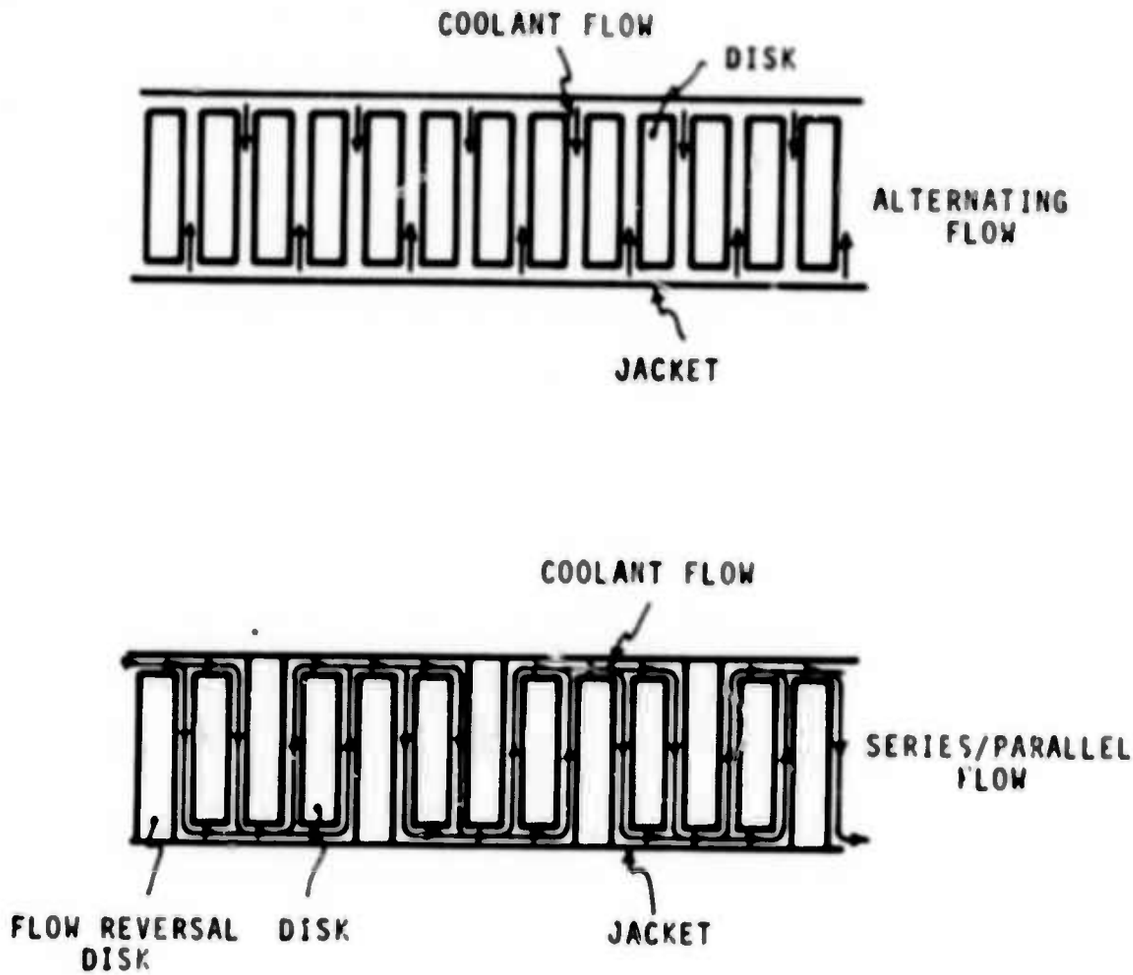

Figure 1. FLOW PATHS FOR ELIMINATING INDUCED OPTICAL WEDGE

order to minimize beam distortion from these effects one can simply restrict the beam to the center of the disk[4]. The device efficiency, however, will suffer. These edge distortions, and they aren't really very large, can be tolerated for some applications. Heat flow in the radial direction can be reduced considerably by cladding the disk with a low thermal conductivity material. Conventional cladding techniques, however, themselves introduce stresses into the disk, and are not completely effective in eliminating radial heat flow[4,6].

Good cavity design can reduce all of the sources of radial heat flow to tolerable limits except that at the edge of the disk. Other researchers have experimented with various cladding techniques. Their approach was to cast the laser disk in a transparent medium[6]. UV Plexiglas had the required transmission and resistance to UV radiation, but was too rigid and stressed the disk. They were unable to solve this problem and decided to tolerate the edge effects.

A new approach to this problem has produced promising results which could reduce beam distortions resulting from these edge effects by a factor of five[7]. This new technique involves bonding the laser disk into a disk holder with FEP Teflon(R). FEP Teflon(R) is ideally suited for this purpose. Its transmission is flat (at over 90%) from about 2000Å to nearly 4μ. It is flexible at room temperature so that it will not allow stresses to be established in the laser disk as a result of the bonding process. Fabrication costs should be less than those for glass clad disks since small mismatches between the disk to cladding surfaces can be accommodated by the Teflon(R).

A program has been carried out whose dual purpose was to investigate the possibility of using:

1) FEP Teflon(R) as a transparent solder to hold the laser disk; and,

2) YLF doped with Ho^{3+} in a sliced laser configuration to obtain high average power at two microns.

The results of this program are summarized in the two sections which follow. The design of the disk laser and fabrication and testing of the laser are presented in that order.

Section 2

DESIGN OF THE DISK LASER

2.0 INTRODUCTION

The design phase of this program indicates that a CW Ho^{3+}:YLF laser is a feasible approach to high average powers at 2μ. The CW threshold of the Ho:YLF disk laser was computed to be about 22 W/cm^3 (about ten times that of usual Nd:YAG laser device[10]). CW output powers of about 6 $watts/cm^3$ are theoretically possible at a pumping rate of 34 $watts/cm^3$*. Repetitively Q switching at 50Hz yields predicted peak powers of $300MW/cm^3$ (10 Joules, 30ns).

Two approaches for generating high CW powers at 2μ have been investigated and evaluated. A CW room temperature Ho:YLF disk laser is discussed first. Pumping rates, fracture limits, oscillation thresholds and laser outputs are computed for this device. An amplifier for a low power CW laser is then discussed as an alternative approach to room temperature generation of a high power, CW, 2μ, laser beam. Both single stage and multistage amplifiers are discussed for both CW and pulsed amplifiers.

2.1 CHARACTERISTICS OF A CW ROOM TEMPERATURE Ho:YLF DISK LASER

Since the threshold of a quasi three level device will be high, an analysis was undertaken first to determine whether it was possible to reach threshold with currently available pump lamps. We must, therefore, determine the pumping rate available at the disk and compare it with the pumping rate required for threshold. The disk geometry must be capable of handling the expected power levels without fracturing. Since it will be shown that the pumping rate exceeds threshold, laser output can be generated and estimates are made.

---

*The pumping rate is the rate at which ions are being added to the excited state times the energy of the laser transition. See also reference (8).

2.1.1 Pump Power Density At The Disk

The power density at the disk is determined by the geometry of the pump cavity. The volume of the arc will be magnified by its envelope by an amount $(n_{\ell e}/n_{cav})^2$[9] where $n_{\ell e}$ and n_{cav} are the indices of refraction of the envelope and the medium filling the pump cavity (water). The elliptical pump cavity images this magnified arc into an oblong transverse to the major axis of the ellipse. Its dimensions are, roughly, $\{[(a + c)/(a - c)]2r_{\ell e}\}$ by $[2r_{\ell e}]$ where a and c are the usual ellipse parameters and $r_{\ell e}$ is the magnified radius of the pump lamp. Given the power density inside the lamp (P_ℓ/V_ℓ) and the fraction of this power density which could become fluorescence, n_{power}, then the power density at the disk, U_ℓ'', will be[9]

$$U_\ell'' = \left(\frac{a - c}{a + c}\right)\left(\frac{n_{cav}}{n_{\ell e}}\right)^2 \left(n_{power}\right)\left(\frac{P_\ell}{V_\ell}\right) E.$$

Typical values for the parameters are:

$a = 2.0cm$

$c = 0.77cm$

Pump Cavity Efficiency $E = 0.74$

$n_{cav} = 1.33$ (water)

$n_{\ell e} = 1.47$ (quartz)

$n_{power} = 0.06$

$P_\ell/V_\ell = 2000\ W/cm^3$ (EG&G arc lamp Model #FX111C - 3.0)

We find, therefore, that

$$U_\ell'' = 34\ W/cm^3.$$

2.1.2 CW, Room Temperature Ho:YLF Threshold

The threshold, U_{th}, for this laser is determined from (8)

$$U_{th} = \left(\frac{B_8 n_o + \Delta N_{th}}{B_7 + B_8}\right) W$$

where

B_7 and B_8 are the fractional populations of the upper and lower laser levels;

ΔN_{th} is the population inversion required to overcome laser cavity losses;

$W = \frac{h\nu}{t_{sp}}$ is power associated with a spontaneously decaying laser photon; and,

n_o is the active ion doping level.

Since neither the doping level nor the threshold is known we cannot procede without determining one or the other. An upper limit on the doping level can be found by setting the threshold equal to the pumping rate

$$U_{th} = U_{\ell}"$$

and noting that,

$$\Delta N_{th} = \frac{1}{\sigma}\left\{\alpha - \frac{\ell n(1 - t_o)}{2\ell_m}\right\},$$

$$\Delta N_{th} = 4.73 \times 10^{17}/cm^3,$$

where

$0.05/cm = \alpha$ is the loss coefficient in the laser medium;

$1.2 \times 10^{-19} cm^2 = \sigma$ is the cross section for stimulated emission at the laser line peak;

$0.1 = t_o$ is the output coupling; and,

$7.5cm = \ell_m$ is the length of the laser medium.

A minimum value of n_o is the population inversion required to overcome cavity losses, ΔN_{th}. An analysis of this sort (in Appendix A) indicates that the doping level must lie in the range

$$0.0473 \times 10^{19} < n_o < 2.6 \times 10^{19}$$

A value of $n_o = 10^{19}$ ions/cm^3 has been selected as a suitable compromise and will require a pumping rate 22 W/cm^3 at threshold. This value of the threshold, incidentally, is about ten times that of Nd:YAG lasers[10].

2.1.3 Thermal Fracture Considerations

An analysis of fracture limits for solid rods and disks indicates that this pumping rate can be (see ref. 5) sustained in a Ho:YLF disk whose dimensions are:

diameter = 10mm

thickness = 3.17mm

An inter-disk spacing of 0.3mm will assure adequate flow rates and a low pressure drop across the disk assembly.

2.1.4 Ho:YLF Disk Laser Output

The laser output for any type of laser system (four level, quasi three level or three level, arc lamp or flashlamp pumped) can be predicted by the following equation[8]:

$$U_o = U_{eff}\left(1 - \frac{1}{\sqrt{\phi}}\right)^2$$

where

U_{eff} is the effective pumping rate of the upper laser level; and,

ϕ is the threshold ratio.

The threshold ratio is simply the ratio of the effective pumping rate to the pumping rate at threshold (zero output coupling)[8]. The effective pumping rate is the actual pumping rate less that required to equalize the populations of the two laser levels. In the special case of a four level laser the effective pumping rate is the actual pumping rate. For the Ho:YLF laser under consideration

$$U_\ell'' = 34 \text{ W/cm}^3$$

and so,

$$\phi \approx 7.5.$$

Therefore

$$U_o \approx 6 \text{ W/cm}^3.$$

If this laser were repetitively Q switched at $f = \frac{1}{t_{sp}} = 50\text{Hz}$ the predicted peak power will be around 326 MW/cm^3[8]. This number, of course, seems rather large. The pulse width predicted for this pulse is about 30ns[11] corresponding to a pulse energy of 10J/cm^3. The small signal gain coefficient for the threshold ratio of 7.5 is[8]

$$g_o = \alpha\sqrt{\phi} = 0.137/\text{cm}.$$

2.2 CW, ROOM TEMPERATURE Ho:YLF DISK AMPLIFIER

An alternative approach for generating a high power CW 2μ beam is to amplify the output of a low power laser. We shall review, briefly, the pertinent equations for laser amplifiers as derived in[12]. Both single and multistage amplifiers will then be discussed whose operational parameters are the same as those of the

laser considered in Section 2.1. As with a laser, we can optimize the operation of an amplifier. The design parameters of such an optimized amplifier are, therefore, computed. It will be seen that a CW amplifier is not a very efficient way to generate high CW power levels. It is, however, an accepted technique for amplifying the output of a flashlamp pumped laser to high energy levels.

2.2.1 Amplifier Equations

The amplifier equations for a homogeneously broadened gain curve which are pertinent to our discussion of Ho:YLF amplifiers are:

1) The relationship between the input and output and the gains and losses is expressed by[12]

$$\alpha\left(\frac{g_o}{\alpha} - 1\right)\ell = \ell n\left(\frac{\beta_2}{\beta_1}\right) - \left(\frac{g_o}{\alpha}\right) \ell n \left[\frac{\frac{g_o}{\alpha} - 1 - \beta_2}{\frac{g_o}{\alpha} - 1 - \beta_1}\right]$$

where

$\beta_{1,2} = \frac{I_{1,2}}{I_s}$ is the normalized input (1) and output (2) beam intensity;

I_s is the saturation intensity;

g_o is the small signal gain coefficient (cm^{-1}); and,

α is the loss coefficient (cm^{-1}).

2) The maximum beam intensity which can be generated by an amplifier is

$$\beta_{max} = \frac{g_o}{\alpha} - 1.$$

The intensity cannot increase beyond this value since scattering losses, absorption, etc. consume all the additional flux generated in the amplifier.

2.2.2 Single Stage CW Amplifier

The equation in 1), above, allows us to design a single stage amplifier which will increase the power in the beam by an amount ΔP, where,

$$\Delta P = \delta I_s A$$

where

$$\delta = \beta_2 - \beta_1 = \frac{I_2}{I_s} - \frac{I_1}{I_s} .$$

If

$$\frac{\delta}{\beta_1}, \frac{\delta}{\beta_2}, \frac{\delta}{\beta_m} << 1$$

then the trancendental equation in 1) relating δ and β_1 takes the much simpler form:

$$\delta = \frac{(\alpha \ell \beta_1)(\beta_m - \beta_1)}{(\beta_1 + 1)} . \quad (\delta << 1)$$

δ can be maximized with respect to β_1 and we find that δ is maximum when

$$\beta = \beta_{opt} = \sqrt{\frac{g_o}{\alpha}} - 1.$$

The maximum value of δ is

$$\delta_{max} = \alpha \ell \beta_{1\ opt}^2 .$$

For $g_o = 0.137$cm and $\alpha = 0.05$/cm we find that

$$\beta_{1\ opt} = 0.655.$$

If the disk assembly for the CW laser described in Section 2.1 and shown in Figure 2 is now used as a single amplifier stage then

$$\ell = 5.7\text{cm}$$

and so

$$\delta_{max} = 0.122.$$

Since $\frac{\delta_{max}}{\beta_m}, \frac{\delta_{max}}{\beta_1} << 1$, our simple equation for δ will accurately predict δ given β_1. For $\delta_{max} = 0.122$, the maximum power increase will be

$$\Delta P_{max} = 2.87 \text{ watts}$$

for an input power of

$$P_{in} = \beta_{1\ opt} I_s \pi r_d^2 = 14.5 \text{ watts.}$$

Letting ρ be the ratio of the power out to the power in

$$\rho = \frac{P_{in} + \Delta P_{max}}{P_{in}}$$

then

$$\rho = 1.2$$

for this CW amplifier.

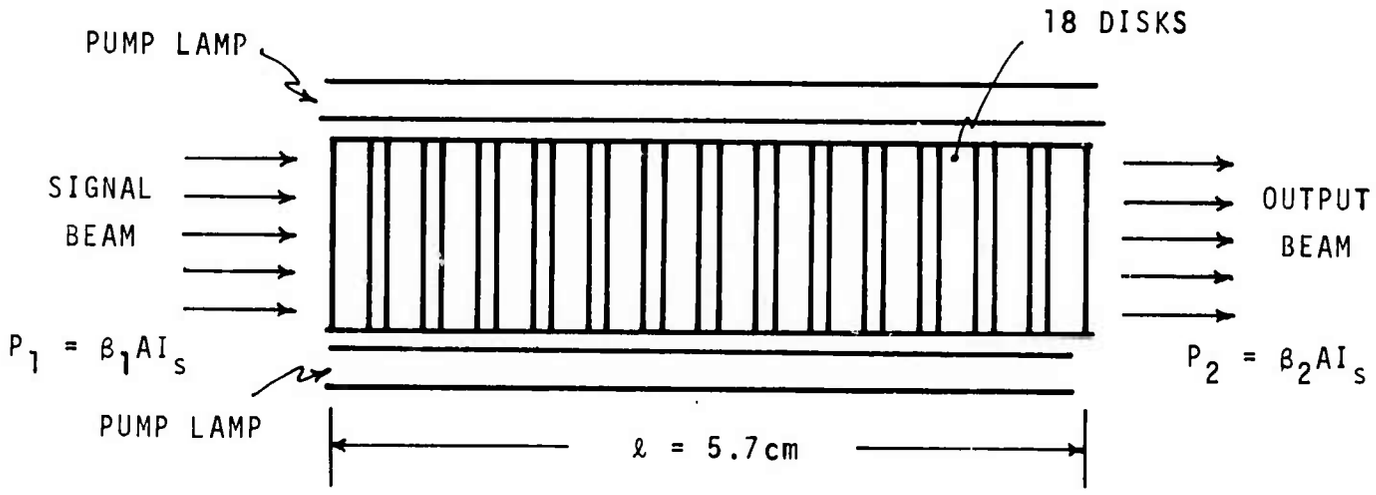

α = 0.05/cm

g_o = 0.137/cm

β_{max} = 1.74

ℓ = 5.7cm

r_d = 0.5cm

Figure 2. EXAMPLE OF Ho:YLF DISK SINGLE STAGE AMPLIFIER

2.2.3 Multistage CW Amplifier

Long amplifiers are not efficient due to saturation effects. Further amplification is possible, however, if the beam is expanded prior to a second amplifier stage and so on. If each disk of the assembly described above is an amplifier stage, then reducing the beam intensity to $\beta_{1\ opt}$ prior to entry into each disk will allow a maximum gain per stage. This reduction in intensity can be easily effected by expanding the beam.

Again using the approximate equation for the power increase

$$\delta_{max} = \alpha \ell \beta_{1\ opt}^2$$

we find that

$$\delta_{max} = 6.78 \times 10^{-3}$$

per disk for

$$\beta_{1\ opt} = 0.655.$$

In this calculation the following parameters of the disk laser are used

$$\ell = 0.317 cm$$
$$g_o = .137/cm$$
$$\alpha = .05/cm.$$

Since the increase in beam intensity from each disk is

$$\delta_{max} = 6.78 \times 10^{-3}$$

the total increase by the 18 disks will be

$$\Delta = 18\ \delta_{max} = 0.122.$$

The maximum power gain is given by

$$\Delta P_{max} = AI_s\Delta$$

$$\Delta P_{max} = 2.875 \text{ watts}$$

when the diameter of the last disk is one centimeter. Again we see that the power gain is small.

2.2.4 Pulsed Amplifier

The amplifiers described above make poor CW amplifiers simply because the gain is so low that the beam intensity never even approaches the saturation value. A pulsed amplifier, however, can produce much larger small signal gain coefficients. We shall repeat the calculations above for the single and multistage pulsed amplifiers with small signal gain of

$$g_o = 1.0/\text{cm}.$$

Let us first examine a single stage amplifier identical to the one described in Section (2.2.2) except that $g_o = 1.0$ instead of 0.137. It is important to determine whether we must use the exact (trancendental) equation relating δ and β_1 or whether the approximate equation for δ_{max} can be used. The simplified equations for β_{opt} and δ_{max} yield

$$\beta_{opt} = 3.47$$

and

$$\delta_{max} = 3.44,$$

and so

$$\frac{\delta_{max}}{\beta_1} = 1.3.$$

Certainly this ratio is not much less than unity, so that the exact equation must be used. When this trancendental equation is solved for δ_{max}, we find that

$$\beta_{1\ opt} = 2.40$$

and that

$$\delta_{max} = 3.37.$$

Thus

$$\Delta P_{max} = 7.95 \text{ watts}$$

for

$$P_{in} = 5.65 \text{ watts}$$

where we are now referring to watts for average power. The ratio, ρ, of power out to power in is

$$\rho = \frac{P_{in} + \Delta P_{max}}{P_{in}}$$

$$\rho = \frac{13.60}{5.65}$$

$$\rho = 2.4.$$

For a multistage pulsed amplifier similar in design to the CW amplifier of Section 2.2.3 we now have

$$g_o = 1.0/cm$$

and so

$$\beta_{1\ opt} = 3.47$$

and, from the approximate equation for δ_{max},

$$\delta_{max} = 0.19.$$

Therefore

$$\frac{\delta_{max}}{\beta_{1\ opt}} \ll 1,$$

and the simplified equation for δ_{max} can be used for each stage with little error.

The increase in the flux from disk-to-disk will require that the beam be expanded in order that the input to each disk remain at $\beta_{1\ opt}$. The area increase per section is

$$\left(\frac{\delta_{max}}{\beta_{1\ opt}}\right) A_d = \Delta A$$

where A_d is the area of the disk the beam has just left.

The total area increase of the beam will be

$$\left(\frac{A_{final}}{A_{initial}}\right) = \left(1 + \frac{\delta_{max}}{\beta_{1\ opt}}\right)^{18}$$

$$\frac{A_{final}}{A_{initial}} = \left(1 + \alpha \ell \beta_{1\ opt}\right)^{18} = 2.61.$$

The total average power increase, δ, for the 18 amplifier stages is

$$\rho = \left(\frac{\beta_{opt} + \delta_{max}}{\beta_{opt}}\right)\left(\frac{A_{final}}{A_{initial}}\right)$$

$$\rho = \left(1 + \alpha \ell \beta_{1opt}\right)^{19}$$

$$\rho = 2.72.$$

The multistage amplifier results in a higher power increase ratio mainly due to expansion of the beam through the assembly.

2.2.5 Summary of Ho:YLF Amplifier

Flashlamp pumped amplifiers are more efficient than CW amplifiers because of the large gain coefficients which can be produced. Furthermore, the disk amplifier lends itself quite naturally to high gain devices where the beam must be expanded to prevent saturation. Figure 3 shows that the diameter of successive disks can be easily increased to match the expanding beam envelope as it passes through the device. The doping level in each disk can be adjusted to optimize the pumping rate. Furthermore, it will be shown in Section 3.1 that tapering the circumference of each disk not only allows an even closer match between the disk and beam envelopes but also provides a means for mounting the disks inside the disk holder.

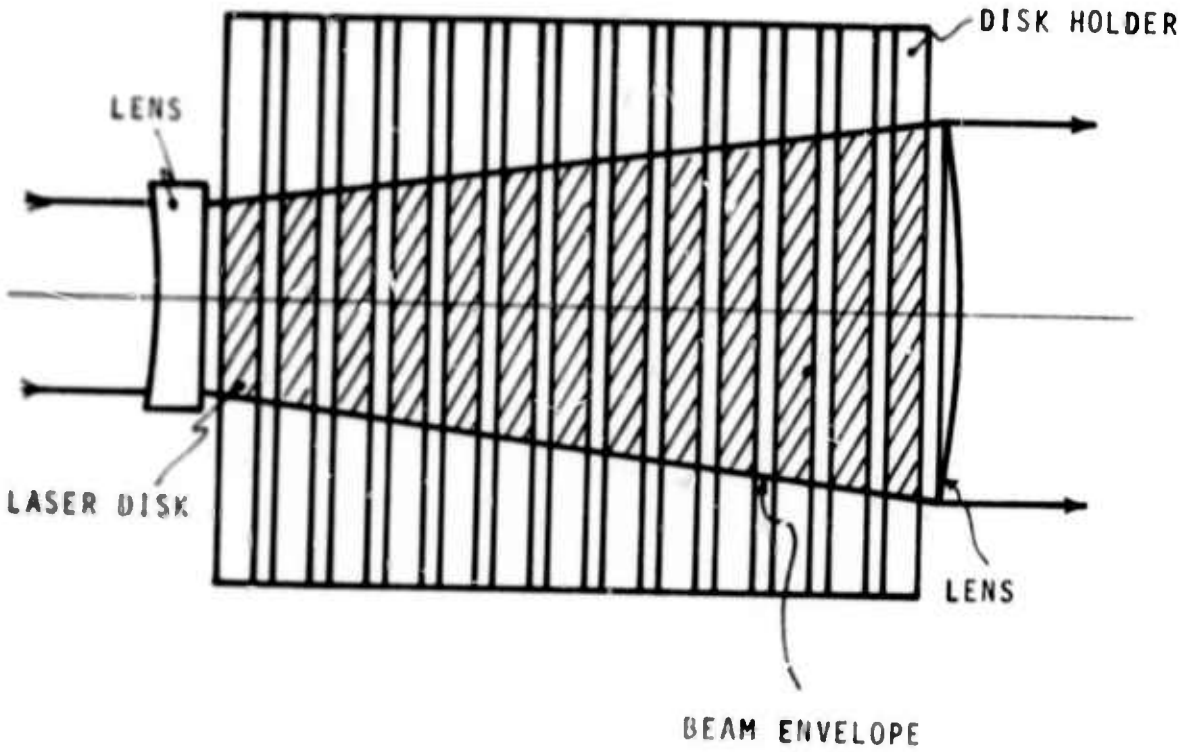

Figure 3. DISK LASER AMPLIFIER.

Section 3

FABRICATION AND TESTING

3.0 INTRODUCTION

A disk laser similar to the one described above has been built and tested. Both fabrication and testing have two major subdivisions. The initial effort in the fabrication phase of this program was to find a practical method to bond the laser disks into the holders. Once this was done the remainder of the laser could be built. The individual clad disks were tested for stresses introduced by the cladding process by observing them through crossed polarizers. Thermal lensing and stresses due to pumping were measured for the disk assembly. Because of time limitations, evaluation of the completed laser head involved only non-lasing experiments.

The significant results of this phase of the program can be summarized as follows:

1) A technique for bonding the laser disks into the disk holders with FEP Teflon(R) has been developed whereby their contacting surfaces have complementary tapers. A laser head incorporating many of the good features of current disk lasers has been built.

2) Measurements of the stresses have shown that the cladding causes no stress in the laser disk even when it is clamped in a vice. Pumping Produces stresses near the edge of the disk from the radial heat flow there. Induced optical power has been measured and is about 50% less than that of a comparable disk laser built by other researchers.

3) The performance of Ho:YLF, in an identical configuration, will be better than that of the ED-2 laser glass disks tested. Since Ho:YLF is five times more resistant to thermal fracture than ED-2

laser glass, pumping rates of 7KW per inch can be sustained by the YLF disks. Optical distortions less than one fifth those in ED-2 laser disks are to be expected in Ho:YLF due to its higher thermal conductivity. Furthermore, if a thick teflon section is used to hold the YLF disk in place, an order of magnitude improvement over glass can be expected in beam quality.

A major change in the program plan was made when it was learned that suitable quantities of Ho:YLF material would not be available in time for their use on this program. In order to obtain some meaningful results, Nd:Glass was substituted as the laser medium. The characteristics of the bonded glass disks could be evaluated and the performance of the Ho:YLF could be, at least, estimated. Because of this delay active laser experiments could not be carried out on the program.

3.1 FABRICATION OF THE BONDED DISKS

A detailed discussion of the bonding technique was the topic of the semi-annual report for this program[7]. The major results of this report are summarized below.

Because of the high temperatures and external forces required to bond with FEP Teflon(R), a novel approach for inserting the disk in the disk holder was required*. Experiments showed that a satisfactory bond could be achieved if both the disk and holder were tapered on their contacting surfaces. Twenty two disks and disk holders were fabricated in this manner - twenty with Nd:Glass disks and two with Ho:YLF disks.

3.1.1 Fabrication of The Laser Head

Many good features of other disk lasers have been incorporated into this device. The pump cavity is a dual lamp clamshell configuration allowing easy access to the disk tray and other cavity components.

*A patent disclosure has been submitted for this technique.

The two cavity halves are flooded with water for both lamp and cavity cooling. The disk tray is a sealed unit permitting coolants other than water to be used without contamination. The coolant flow direction alternates from flow channel to flow channel to eliminate beam walkoff. Furthermore all flow channels for flow in one direction are connected in parallel to keep the system pressures low and the flow rates high. Typical flow parameters are:

Total flow	2-1/2gpm
Flow per channel	0.13 gpm
Total pressure drop (including lines to laser head)	12 psi

The total temperature rise across the disk assembly was about 3°C for 4KW average power into the 18 Nd:Glass disks. Photos of the laser head are shown in Figure 4.

3.2 TESTING - NON-LASING

Non-lasing experiments with the laser head included observations of the induced stresses and measurements of the induced optical power in the disks.

3.2.1 Cladding Induced Stresses

The major drawback of conventional cladding techniques - stress in the clad disk - is eliminated by bonding the disk in the cladding material with teflon. No stresses could be observed in the disk even when the disk holder was clamped in a vise (see photos, Figs. 5 and 6).

3.2.2 Induced Effects Due to Pumping - Stress

Two induced effects - stresses and thermal lensing - result from pumping. Both are due to heat flowing radially in the disk.

If the pumped disks are observed through crossed polarizers stress is observed near the circumference of the disk (see Fig. 7). These stresses are similar to those observed in solid rods.

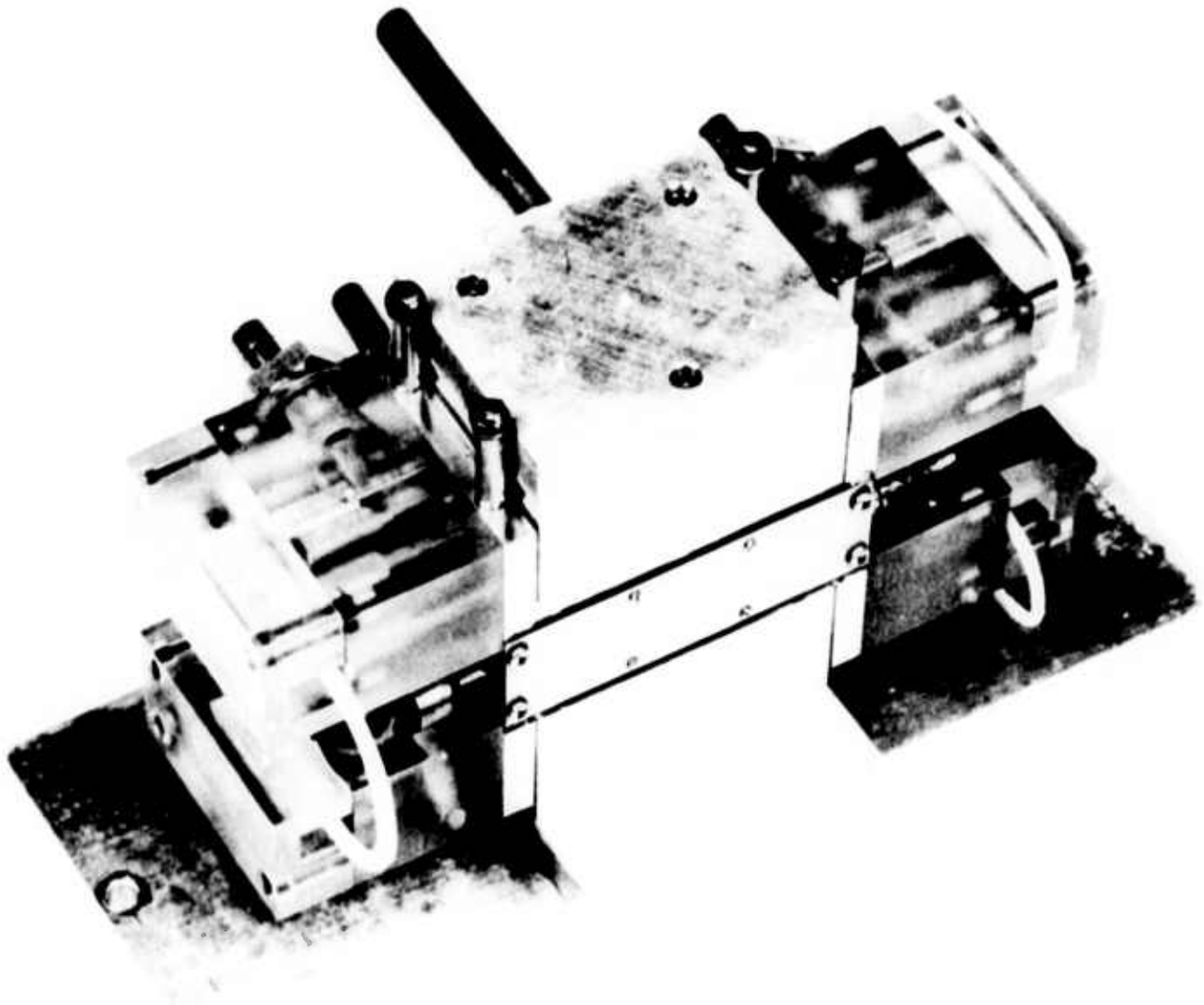

Figure 4a. COMPLETE DISK LASER HEAD

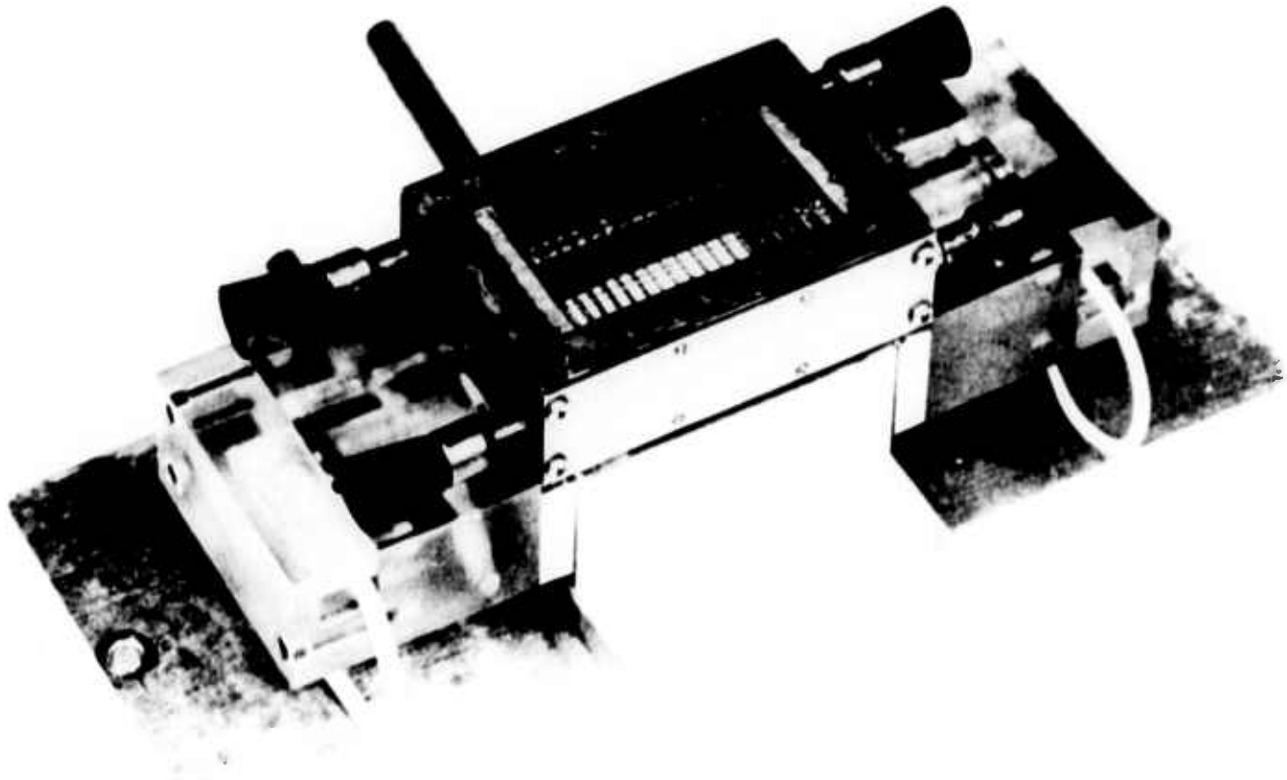

Figure 4b. DISK LASER WITH TOP CAVITY HALF REMOVED TO SHOW DISK TRAY.

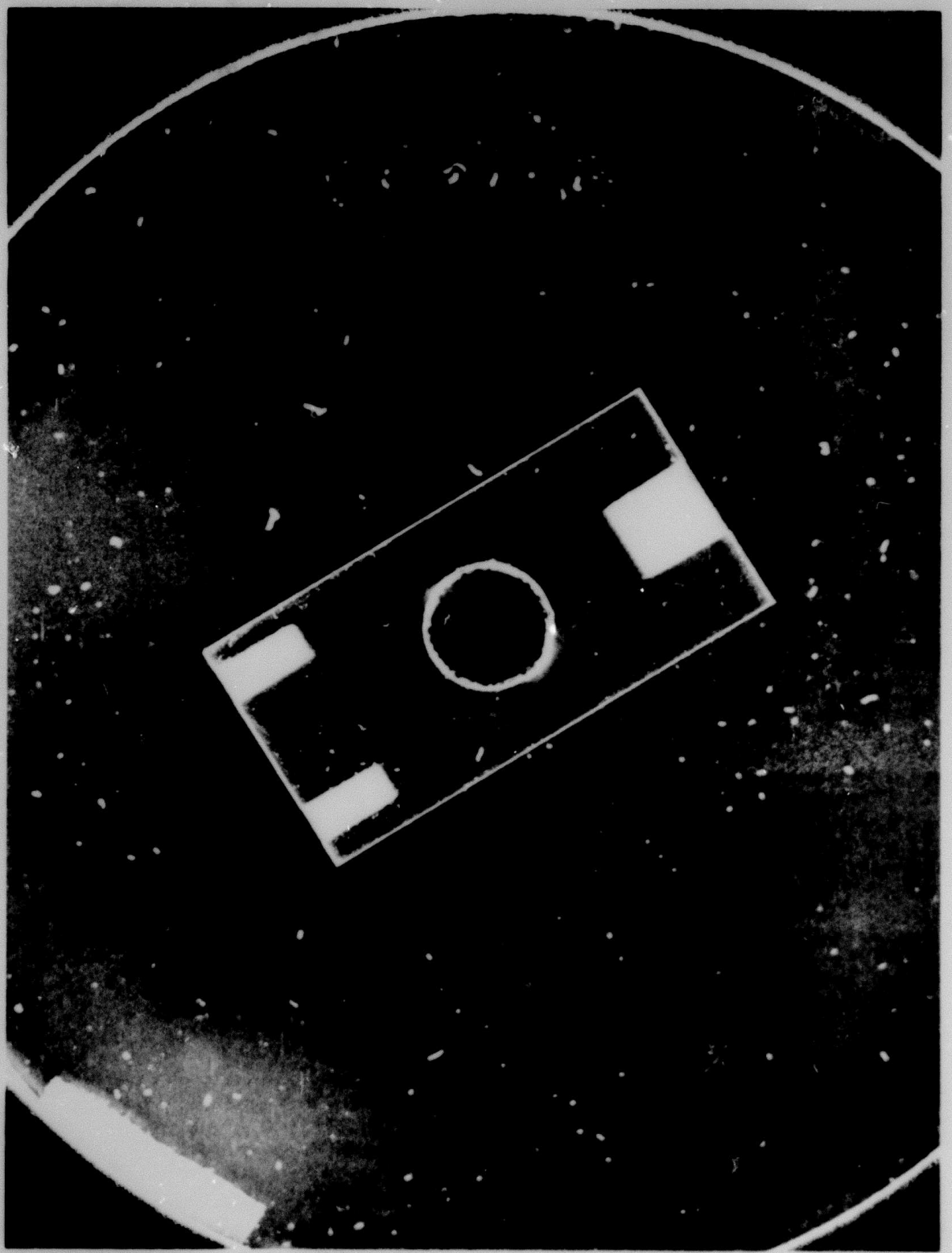

Figure 5a. GLASS DISK - UNCLAMPED

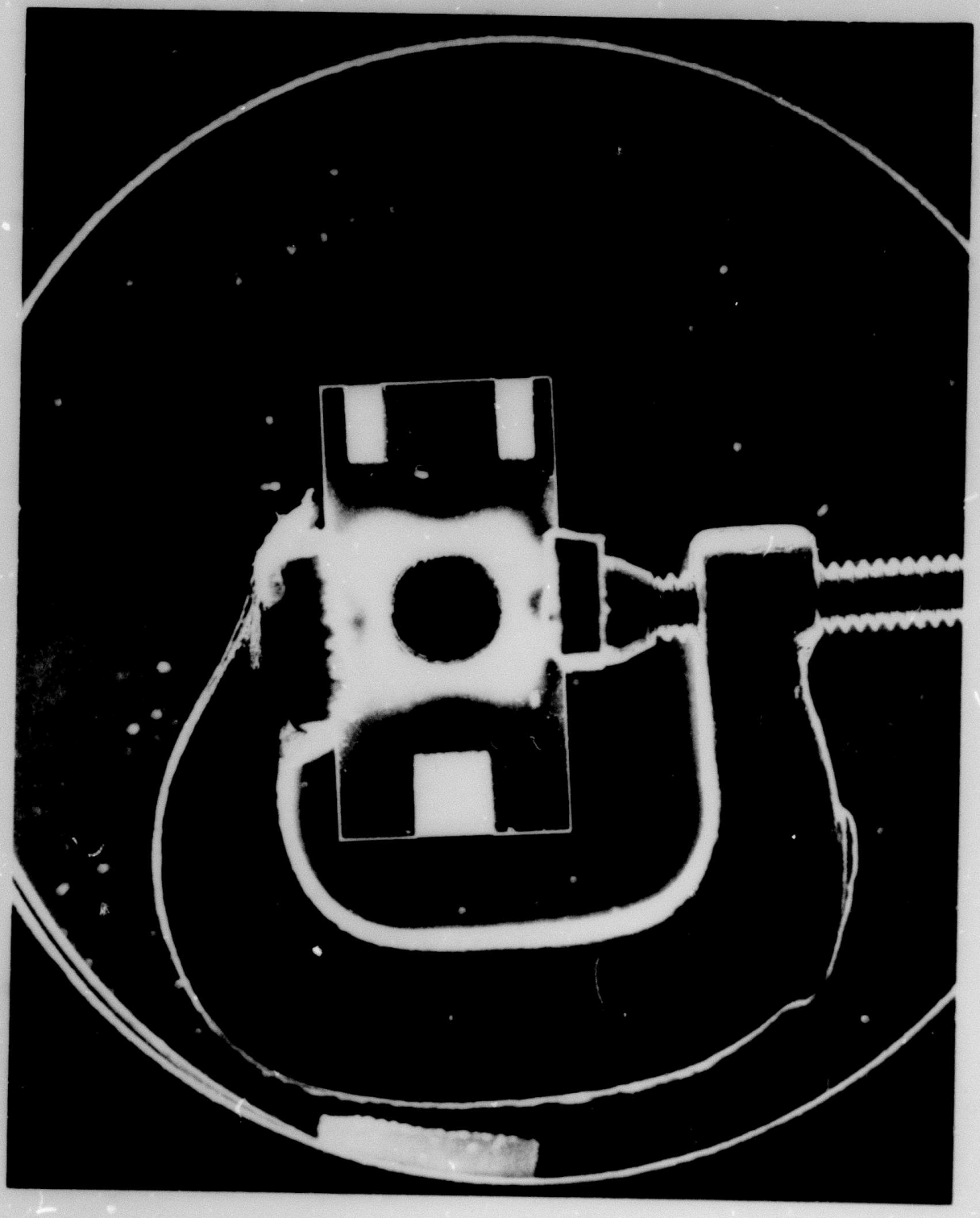

Figure 5b. GLASS DISK - CLAMPED

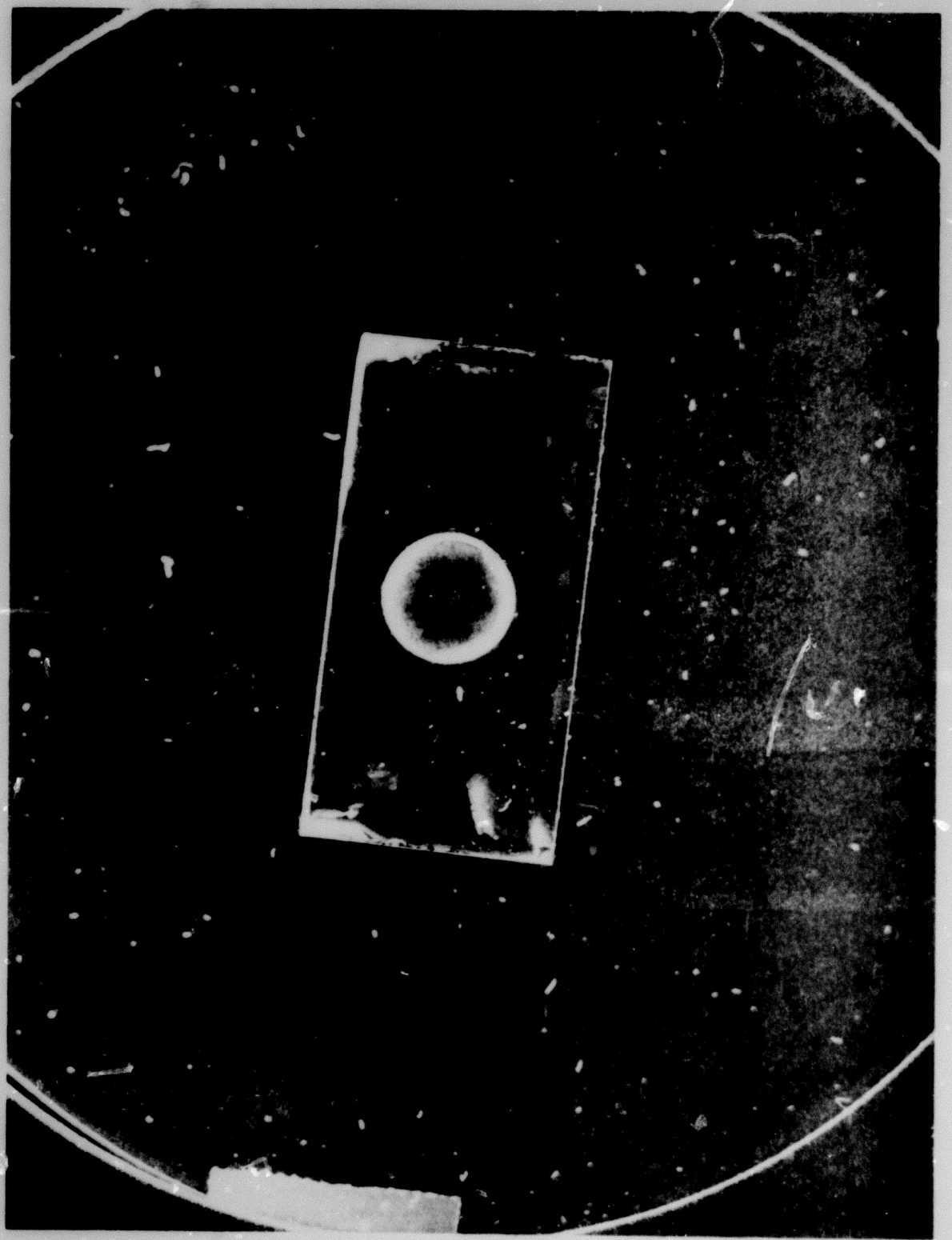

Figure 6a. YLF DISK - UNCLAMPED

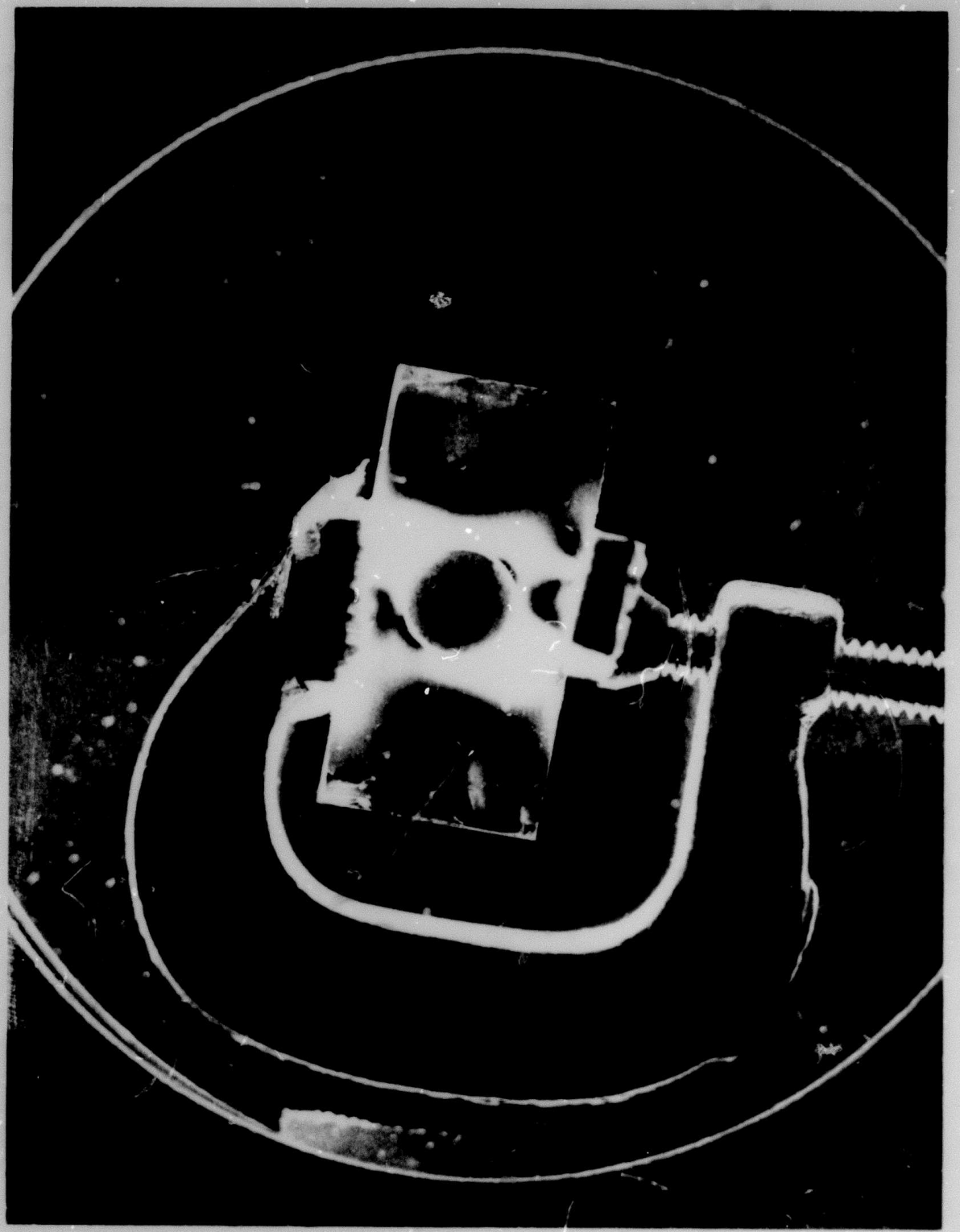

Figure 6b. YLF DISK - CLAMPED

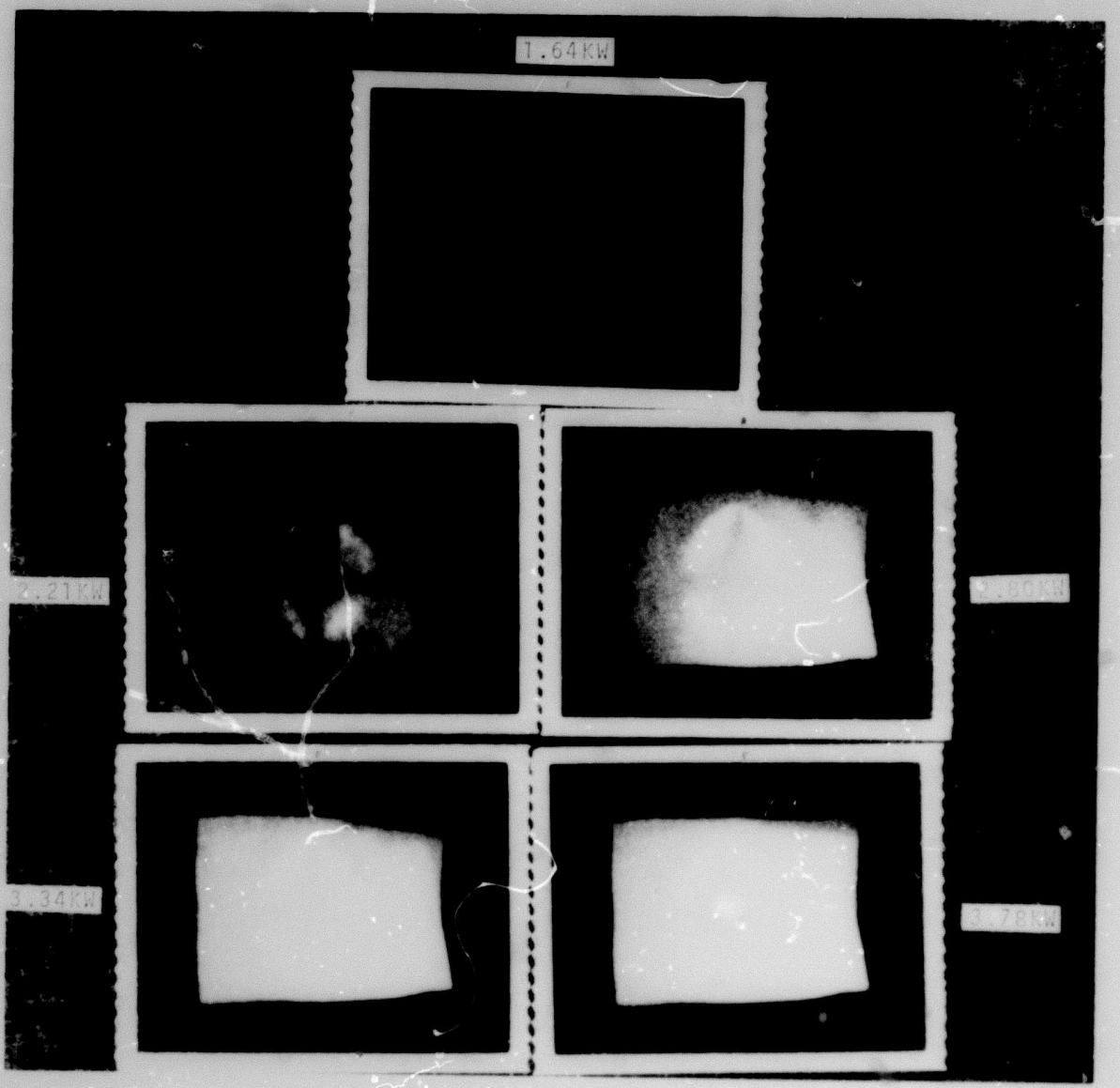

Figure 7A-7E. PUMPED DISK OBSERVED THROUGH CROSSED POLARIZERS

THIS PAGE PURPOSELY LEFT BLANK

3.2.3 Induced Effects Due to Pumping - Thermal Lensing

A comparison of the induced thermal lensing of the S/A disk laser with that reported in reference (6) is given by the graph in Figure 9. It can be shown (Appendix B) that if the ratio of the measured optical powers is

$$\frac{\frac{1}{f}\Big|_{SA}}{\frac{1}{f}\Big|_{(6)}} = \frac{\left(\frac{\eta_{cav}\,\ell}{r_d^2}\right)_{SA}}{\left(\frac{\eta_{cav}\,\ell}{r_d^2}\right)_{(6)}} = 1.377$$

then the two lasers have equivalent induced thermal lensing properties. If this ratio of observed thermal lensing is less than 1.377, then the S/A disk laser has less induced lensing than does the disk laser of reference (6). The induced thermal lensing measured for both lasers is plotted in Figure 9 along with the ratio

$$\left(\frac{\frac{1}{f}\Big|_{SA}}{\frac{1}{f}\Big|_{(6)}}\right)_{observed}$$

At high pumping rates this ratio approaches 0.622. Since this ratio is about half that predicted for equivalent induced lensing, it must be concluded that the S/A disk laser has approximately half the induced lensing of the laser of reference (6).

The larger thermal lensing of reference (6) can be attributed, at least in part, to heat flowing radially near the circumference of the disk. The Nd:Glass core of this laser was clad with a samarium doped glass. The thermal properties of the cladding are, most likely, the same as those of the laser glass to eliminate stress problems.

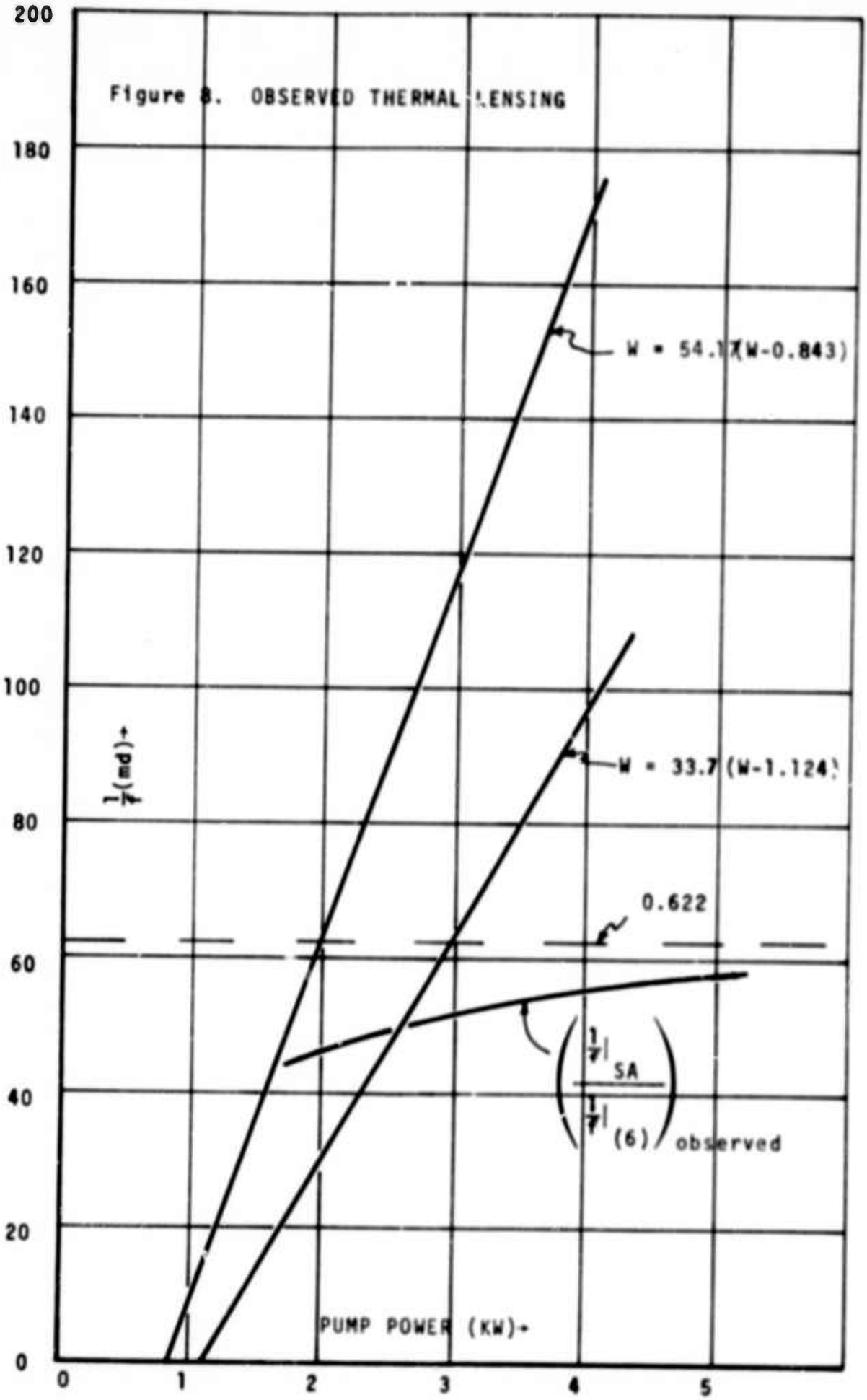
Figure 8. OBSERVED THERMAL LENSING
200
180
160
140
120
100
80
60
40
20
0
0
1
2
3
4
5
W = 54.1(W-0.843)
W = 33.7(W-1.124)
0.622
$\frac{1}{f}$(md)+
PUMP POWER (KW)+
$\left(\frac{\frac{1}{f}|_{SA}}{\frac{1}{f}|_{(6)}}\right)_{observed}$

The Nd:Glass disks in the S/A laser, however, were bonded into holders whose thermal conductivity is less than that of the laser disk. Consequently there will be less radial heat flow in our disk laser than in that of reference (6). An analysis of the heat flow near the edge of the disk (see Appendix C) indicates that the ratio of radial heat flow in the S/A disk laser to that of reference (6) is:

$$R = 0.71.$$

Better agreement between this ratio and the observed ratio of thermal lensing (≈ 0.5) for the two lasers is not possible as the details of the holding technique for the laser of (6) are not known.

Section 4

RECOMMENDATIONS FOR DISK LASER DESIGN

The brightness of disk lasers can be improved by mounting the disk in a holder whose thermal conductivity is much less than that of the disk itself. The use of FEP Teflon(R) to bond the laser disk into the disk holder allows a wide choice of disk holding materials. By selecting a holder material whose thermal conductivity is much lower than that of the disk, a much higher thermal isolation of the edge can be achieved than is now possible.

Section 5

SUMMARY AND CONCLUSIONS

This bonding technique presents a wider choice of cladding materials to the disk laser designer. It will allow, perhaps, a factor of five reduction in beam distortions over conventional glass disk lasers. It allows even high thermal conductivity laser materials to be clad safely without inducing stresses in the laser disk.

Furthermore, the CW room temperature Ho:YLF disk laser is a possibility. High CW powers and high peak powers and pulse energies are predicted. The quasi three level nature of Ho:YLF, however, requires pumping rates nearly ten times that of Nd:YAG just to reach threshold. Improvements in beam quality of an order of magnitude can be expected over current Nd:Glass disk lasers.

APPENDIX A

DETERMINATION OF THE ACTIVE ION DENSITY

The active ion density, n_o, must be determined before calculations of the threshold can be made. The equation for the CW output power[A1]

$$U_o = U''_\ell - U_{th}$$

and the CW threshold[8]

$$U_{th} = \left(\frac{B_8 n_o + \Delta N_{th}}{B_7 + B_8}\right) W$$

allow the maximum active ion density to be computed given U_o, ΔN_{th}, U''_ℓ and the temperature. We can combine these equations in the form:

$$n_{o\ max} = (U''_\ell - U_o)\left(\frac{B_7 + B_8}{WB_8}\right) - \left(\frac{\Delta N_{th}}{B_8}\right),$$

to give the maximum active ion density as a function of the laser parameters.

The largest value of n_o occurs when $U_o = 0$, i.e., when the maximum pumping rate is the threshold pumping rate.

Thus

$$n_{o\ max} = \frac{U''_\ell(B_7 + B_8)}{WB_8} - \frac{\Delta N_{th}}{B_8}$$

(A1) A. Yariv & J.P. Gordon, Proc. IEEE, p. 4, Jan. 1963.

The minimum ion density will be many times the population inversion required for threshold. If it happened that the Ho^{3+} ion density were the critical inversion density then 100% of the available ions would have to be inverted just to reach threshold. Since, in Ho^{3+}, the ions in the upper laser level represent about $\frac{1}{B_7 + B_8} \approx \frac{1}{6}$ of those in the excited state manifold (corresponding to 100% of the active ions in the excited state manifold at threshold) will be

$$n_{o\ min} = \frac{\Delta N_{th}}{B_7 + B_8} \approx 6\Delta N_{th} \text{ (at room temperature).}$$

A suitable value of n_o must be much larger than $\approx 6\Delta N_{th} = 0.25 \times 10^{19}/cm^3$ yet less than $n_{o\ max}$. An ion density satisfying both of these conditions is

$$n_o = 10^{19}/cm^3.$$

This value will be used for all calculations where n_o is required. A plot of $n_{o\ max}$ vs t_o is given in Figure A1.

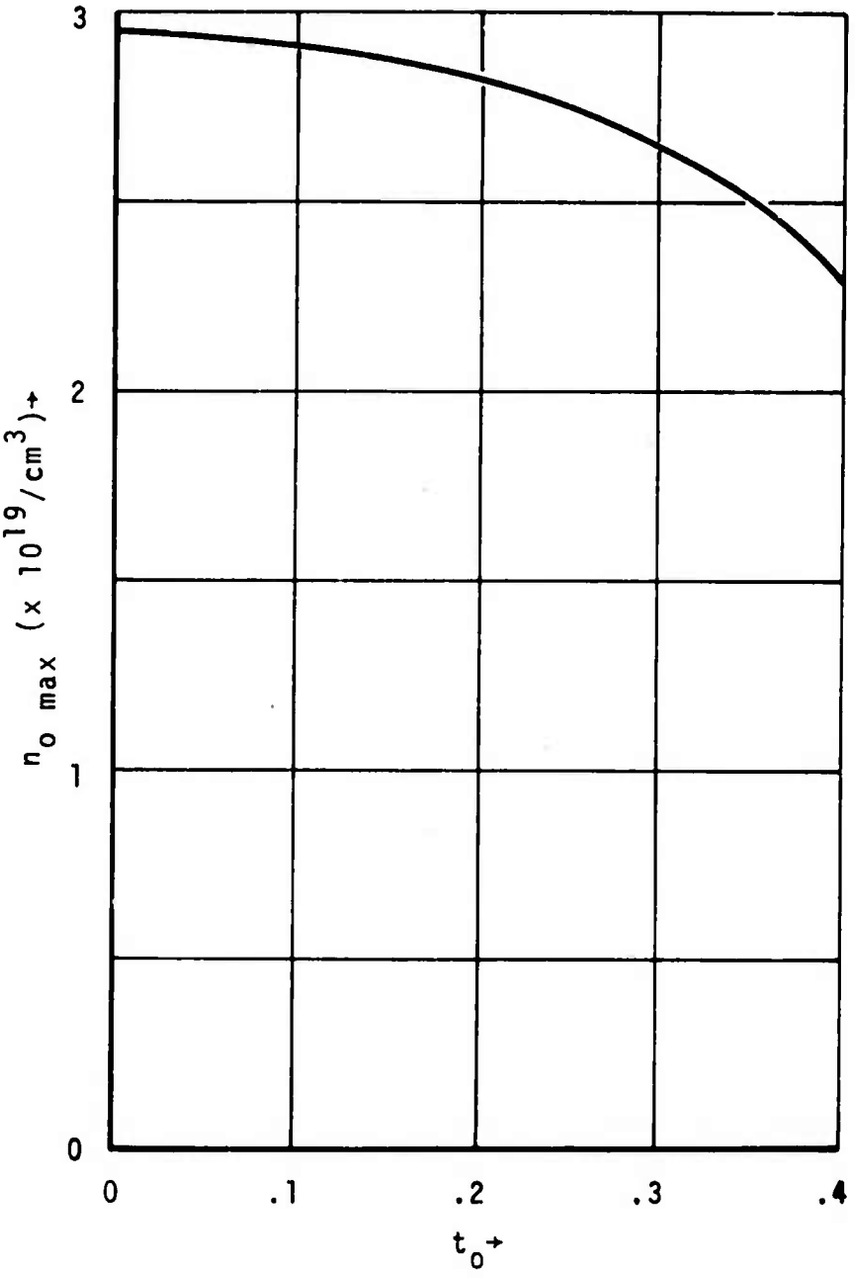

Figure A.1. MAXIMUM ACTIVE ION CONCENTRATION FOR Ho^{3+}:YLF Vs. OUTPUT COUPLING.

APPENDIX B

COMPARISON OF DISK LASERS

In order to compare our measurements of the induced lensing with that of other researchers, we must first normalize our results to account for different pumping rates, disk geometries etc. If we assume uniform thermal loading, then the temperature and, hence, the thermal lensing will be proportional to the thermal loading (W/cm^3). Furthermore, since the induced lensing effects are small, the paraxial ray approximation applies and we can write the effect of N disks as N times that of each disk. Whereas the diameter of the probe beam linearly affects its divergence after passing through the disk assembly, the focal length (and lens power) is independent of the beam diameter. Disk thickness has a large effect on the optical power. Indications are[4] that optical effects depend quadratically on the disk thickness. We, therefore, can summarize the dependence of optical power on the system variables as

$$\frac{1}{f} \alpha U_\ell N \ell^2 = U_\ell \frac{\ell_{assy}}{\ell} \ell = U_\ell \ell_{assy} \ell .$$

The pumping rate, U_ℓ, is computed from

$$U_\ell = \frac{\eta_{cav} P_\ell}{\pi r_d^2 \ell_{assy}}$$

where

P_ℓ is the total lamp power;

η_{cav} is the efficiency of the pump cavity, $\eta_{cav} = 3/4$ for a single elliptical pump cavity, $\eta_{cav} = 2/3$ for a dual lamp cavity, $\eta_{cav} = 1/2$ for a four lamp cavity;

r_d is the disk radius; and,

ℓ_{assy} is the total length of the disk assembly including the coolant passages.

Furthermore, the number of disks, N, is found from

$$N \approx \frac{\ell_{assy}}{\ell + d}$$

where

d is the thickness of the coolant channel.

Usually

$$\frac{d}{\ell} \approx 0.1.$$

or less and we can write

$$N \approx \frac{\ell_{assy}}{\ell} .$$

Consequently,

$$\frac{1}{f} \alpha \frac{\eta_{cav} P_\ell \ell}{r_d^2} .$$

An optical power reported by reference (6) would have to be multiplied by the factor

$$\frac{\left(\frac{\eta_{cav} P_\ell \ell}{r_d^2}\right)_{SA}}{\left(\frac{\eta_{cav} P_\ell \ell}{r_d^2}\right)_{(6)}}$$

to compare it with the data taken for our disk laser. The Nd:Glass laser reported in[6]

η_{cav} = 1/2 (4 lamps)

ℓ = 1.0cm

r_d = 0.9cm

Thus, at equal pumping rates, the ratio of optical powers should be

$$\frac{\left(\frac{n_{cav}\ell}{r_d^2}\right)_{SA}}{\left(\frac{n_{cav}\ell}{r_d^2}\right)_{(6)}} = 1.377$$

If the ratio of the measured optical powers is less than this value, then the difference represents an improvement in induced thermal lensing by the S/A disk laser.

APPENDIX C

RADIAL HEAT FLOW

Some radial heat flow will occur near the circumference of the disk even though it is in contact with a disk holder of low thermal conductivity since it is not the absolute thermal conductivity of the holder which is important but rather its magnitude with respect to that of the disk. Estimates of the relative thermal impedance of the two paths - one from the center of the disk (at the edge) to the coolant ($\overline{AB}$) and the other from the same point in the disk through the disk/holder interface and then to the coolant ($\overline{ACD}$) (See Fig. C1A) can be easily made. The path through the disk holder for the bonded disk has a higher thermal impedance due to the presence of the bonding agent. Thus, all other things being equal, the impedance $\overline{A'C'D'}$ is greater than the impedance of $\overline{ACD}$.

The thermal impedance along rods and through the walls of thin cylinders can be approximated by*

$$R \approx \frac{\Delta L}{Ak} = \frac{\Delta T}{W}$$

where

ΔL is the length of thickness;
A is the area of the rod or cylinder surface; and,
k is the thermal conductivity of the material.

The thermal resistance of $\overline{AB}$ is approximately

$$R_{\overline{AB}} = \frac{x/2}{Ak}$$

*Condon and Odishaw, Handbook of Physics, McGraw Hill, 1958, pp 65-66.

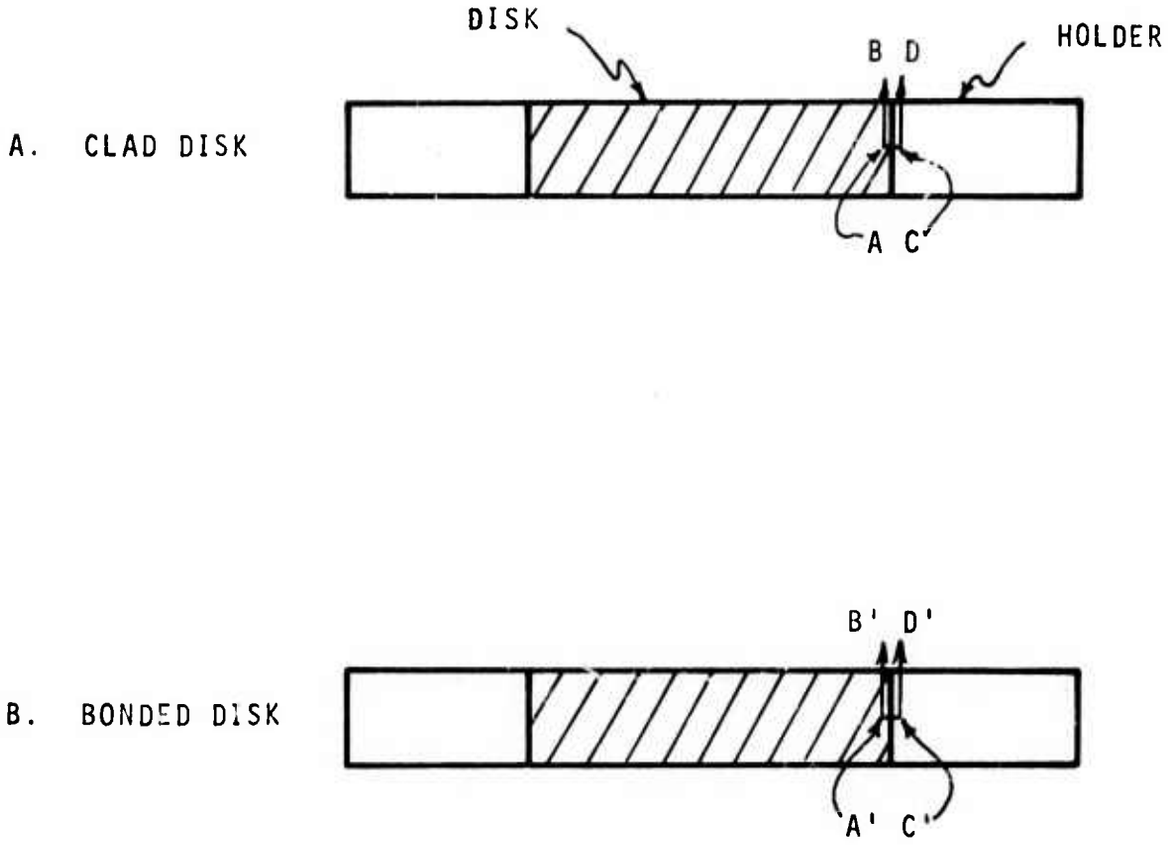

$$R_{th}^{AB} \approx R_{th}^{ACD} \approx R_{th}^{A'C'D'} \approx R_{th}^{A'B'}$$

$$R_{th}^{AC} \approx R_{th}^{A'C'}$$

Figure C.1. HEAT FLOW IN A CLAD DISK

where

$A = 2\pi r_d x$ is a small annular area near the edge of the disk whose width is the same as the thickness of the disk.

Similarly we can find the impedances of $\overline{CD}$, $\overline{A'B'}$ and $\overline{C'D'}$. The impedance of $\overline{A'C'}$ is approximately

$$R_{\overline{A'C'}} = \frac{t}{2\pi r x k} .$$

The relative heat flow along the two paths $\overline{AB}$ and $\overline{ACD}$ is

$$\frac{R_{\overline{AB}}}{R_{\overline{ACD}}} = \frac{\left(\frac{x}{2\pi r dr k_{disk}}\right)}{\left(\frac{x}{2\pi r dr k_{holder}}\right)} = \left(\frac{k_{holder}}{k_{disk}}\right)$$

and along the two paths $\overline{A'B'}$ and $\overline{A'C'D'}$ is

$$\frac{R_{\overline{A'B'}}}{R_{\overline{A'C'D'}}} = \frac{\left(\frac{x}{2\pi x k_{disk}}\right)}{\left(\frac{x}{2\pi r x k_{holder}}\right) + \left(\frac{}{2\pi r x k_{teflon}}\right)}$$

$$\frac{R_{\overline{A'B'}}}{R_{\overline{A'C'D'}}} = \frac{\frac{1}{k_{disk}}}{\left(\frac{1}{k_{holder}}\right) + \left(\frac{t}{x k_{teflon}}\right)} .$$

Since

$x = 0.317\text{cm}$

$t \quad 2.05 \times 10^{-4}\text{cm}$

$k_{disk} \approx 3.01 \times 10^{-3} \frac{\text{cal cm}}{\text{cm}^2 \text{ sec } ^\circ\text{C}}$

$k_{\substack{\text{glass} \\ \text{holder}}} \approx 2.2 \times 10^{-3} \frac{\text{cal cm}}{\text{cm}^2 \text{ sec } ^\circ\text{C}}$

$k_{teflon} = 4.65 \times 10^{-4} \frac{\text{cal cm}}{\text{cm}^2 \text{ sec } ^\circ\text{C}}$

then

$$\frac{l}{k_{holder}} = 450 \frac{cm^2 - sec - °C}{cal} << \frac{k}{xk_{teflon}} = 1.70 \frac{cm^2 - sec - °C}{cal}$$

and it is apparent that the Teflon$^{(R)}$ really provides little thermal insulation, mainly due to its tiny thickness.

The ratio of disk/holder thermal conductivities allow the thermally induced lensing to be estimated if one compares this ratio with that of a disk laser whose lensing characteristics are known. The thermally induced lensing will be, roughly, proportional to the ratio of thermal conductivities for the disk/holder assembly ($R_{A'B'}/R_{A'C'D'}$).

REFERENCES

1) E.P. Chicklis et al, Appl. Phys. Lett., 19, 119 (1971).

2) William S. Martin, "Performance Characteristics of a Face Pumped, Face Cooled Slab Laser, the Zig Zag FPL", G.E. Corporate Research and Development, Technical Report AFAL-TR-71-63, April, 1971.

3) C.G. Young, Proc. IEEE, 57, 1269 (1969), p. 1279.

4) W.F. Hagen et al., "Segmented Nd:Glass Lasers", American Optical Corp., Southbridge, Ma., Technical Report F33615-68-c-1570.

5) E. Matovitch, "The Axial Gradient Laser", Autonetics Division of North American Rockwell Corp., Anaheim, Calif.

6) W.F. Hagen et al., "Segmented Nd:Glass Lasers", American Optical Corp., Southbridge, Ma., Technical Report AFAL-TR-71-303, Feb. 1972.

7) First suggested by Dr. V. Nicolai, see also W.C. Fricke, "Segmented High Average Power Ho:YLF Laser", Semi-annual Report #1, Sanders Associates, Inc., Nashua, N.H., Technical Report No. N00014-72-c-0137, June 1972.

8) R.B. Chesler et al., "A Practical High-Repetition Rate Q-Switched Nd:YAG Laser", Bell Telephone Labs., Murray Hill, N.J.

9) W.C. Fricke, "High Power TEM_{00} Laser Study", Fianl Report for IR&D Program, Sanders Associates, Inc., Oct. 1969.

10) A typical threshold for a 1/4" x 3" Nd:YAG laser rod is about 700W (Tungsten iodide pump, .19" diameter x 3.0" long).

11) W.G. Wagner and B.A. Lengyel, J. Appl. Phys., 34, 2040 (1963).

12) W.W. Rigrod, J. Appl. Phys., 34, 2602 (1963).